

Singlet Oxygen Production by Peptide-Coated Quantum Dot–Photosensitizer Conjugates

James M. Tsay,^{†,||,§} Michael Trzoss,[†] Lixin Shi,[‡] Xiangxu Kong,^{†,||} Matthias Selke,[‡] Michael E. Jung,[†] and Shimon Weiss^{*,†,‡,||}

Contribution from the Department of Chemistry and Biochemistry, Department of Physiology, and California NanoSystems Institute, University of California at Los Angeles, Los Angeles, California 90095, and Department of Chemistry, California State University, Los Angeles, Los Angeles, California 90032

Received January 31, 2007; E-mail: sweiss@chem.ucla.edu

Abstract: Peptide-coated quantum dot–photosensitizer conjugates were developed using novel covalent conjugation strategies on peptides which overcoat quantum dots (QDs). Rose bengal and chlorin e6, photosensitizers (PSs) that generate singlet oxygen in high yield, were covalently attached to phytochelatin-related peptides. The photosensitizer–peptide conjugates were subsequently used to overcoat green- and red-emitting CdSe/CdS/ZnS nanocrystals. Generation of singlet oxygen could be achieved via indirect excitation through Förster (fluorescence) resonance energy transfer (FRET) from the nanocrystals to PSs, or by direct excitation of the PSs. In the latter case, by using two color excitations, the conjugate could be simultaneously used for fluorescence imaging and singlet oxygen generation. Singlet oxygen quantum yields as high as 0.31 were achieved using 532-nm excitation wavelengths.

1. Introduction

Photodynamic therapy (PDT) has emerged as a highly effective treatment for oncological diseases.^{1,2} It relies on the effective localization of photosensitizers (PSs) into tumor tissues and the selective destruction of these tissues with light. PSs such as the FDA-approved Photofrin have been used to selectively destroy tumors after injection and photoexcitation. One mechanism for PDT (type I) involves the excitation of PSs, which causes the generation of free radicals such as $\bullet\text{OH}$ and $\bullet\text{O}_2^-$. These compounds are known to oxidize biomolecules and induce tumor destruction. The other mechanism (type II) behind this process involves excitation of the photosensitizer, subsequent intersystem crossing from its singlet state to triplet state, and finally energy transfer from the photosensitizer's triplet state to oxygen molecules (Figures 1 and 2). This energy transfer converts triplet O_2 to singlet O_2 , a substance known to cause irreversible damage to nucleic acids, enzymes, and cellular components such as mitochondria, plasma, and nuclear membranes, eventually leading to programmed cell death (apoptosis).

As mentioned by Bakalova et al., there are several requirements for effective PDT; optimal PSs should (1) be nontoxic in the absence of irradiation, (2) be able to specifically target

cancer, (3) have efficient energy transfer to O_2 , (4) be easily cleared from the body, (5) be resistant to aggregation, and (6) be photostable.^{1,3} Unfortunately, even the most successful PSs, such as Photofrin, have major drawbacks: poor water solubility, low selectivity, skin phototoxicity, and instability. Furthermore, their excitation wavelengths are not optimal for deep tissue penetration.

Quantum dots (QDs) have been established as powerful and versatile biological imaging probes which have high quantum yields, high photostability, large absorption coefficients, continuous absorption bands for multicolor capability, narrow and symmetric emissions, and many biofunctionalization strategies.^{4–6} Although several examples of employing QDs for photodynamic therapy have been described, their full capabilities have yet to be harnessed. For example, Samia et al. showed QDs can be conjugated nonspecifically to PSs using aluminum phthalocyanine Pc4 which has an alkyl amine group.⁷ This complex was able to undergo FRET, which may be particularly useful in extending the range of excitation of PSs and utilizing the high absorption coefficient of QDs (in comparison to dyes). Unfortunately this complex was not soluble in water and, therefore, was not optimal for biological environments. They measured only a low yield of singlet oxygen generation ($\sim 5\%$) of CdSe QDs in toluene (too low of a yield for practical applications).

[†] Department of Chemistry and Biochemistry, University of California at Los Angeles.

[‡] Department of Physiology, University of California at Los Angeles.

^{||} California NanoSystems Institute, University of California at Los Angeles.

[‡] Department of Chemistry, California State University.

[§] Current address: Department of Physics, University of California at San Diego, La Jolla, California 92093.

(1) Ochsner, M. J. *Photochem. Photobiol.*, **B** **1997**, *39*, 1.

(2) Dougherty, T. J. *Photochem. Photobiol.* **1987**, *45*, 879.

(3) Bakalova, R.; Ohba, H.; Zhelev, Z.; Nagase, T.; Jose, R.; Ishikawa, M.; Baba, Y. *Nano Lett.* **2004**, *4*, 1567.

(4) Michalet, X.; Pinaud, F.; Bentolila, L. A.; Tsay, J. M.; Li, J. J.; Doose, S.; Weiss, S. *Science* **2005**, *307*, 538.

(5) Bruchez, M.; Moronne, M.; Gin, P.; Weiss, S.; Alivisatos, A. P. *Science* **1998**, *281*, 2013.

(6) Chan, W. C. W.; Nie, S. M. *Science* **1998**, *281*, 2016.

(7) Samia, A. C.; Chen, X.; Burda, C. *J. Am. Chem. Soc.* **2003**, *125*, 15736.

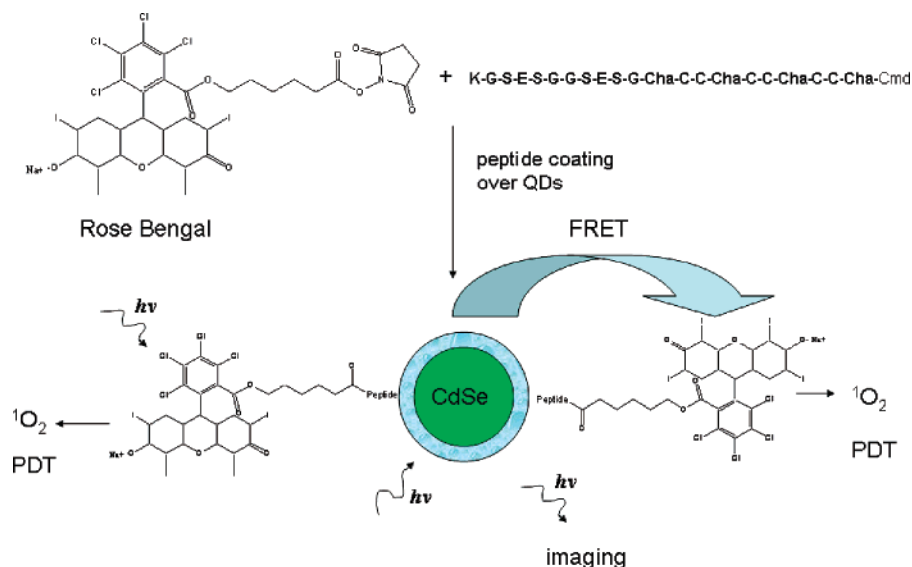


Figure 1. Scheme of the conjugation of rose bengal to peptides used to create QD–photosensitizer conjugates and the proposed mechanisms for singlet oxygen generation

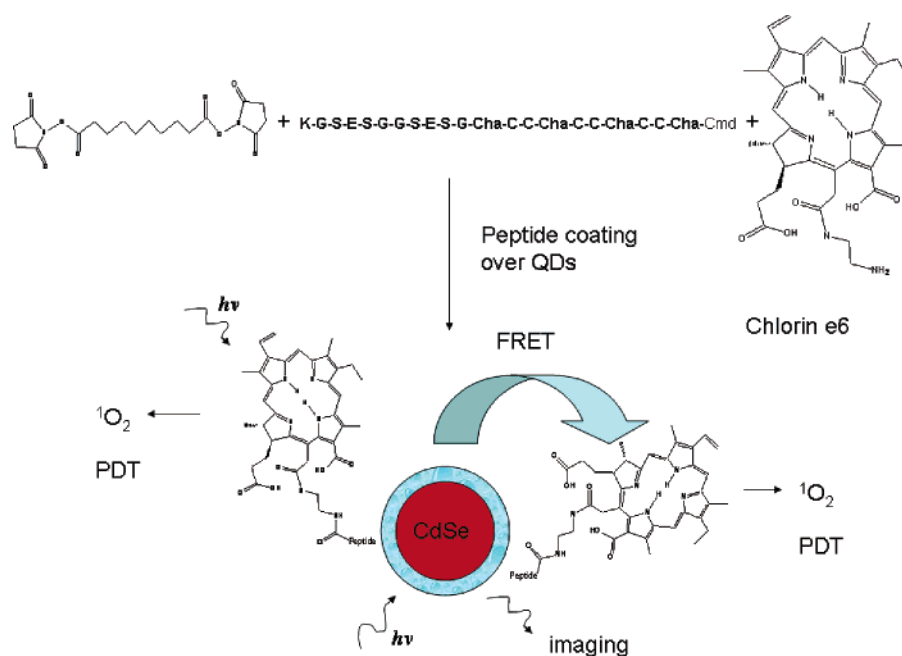


Figure 2. Scheme of the conjugation of chlorin e6 to peptides used to create QD–photosensitizer conjugates and the proposed mechanisms for singlet oxygen generation

Although the inefficiency of QDs alone to generate singlet oxygen is clear, QD–photosensitizer conjugates are still an intriguing option for PDT applications. In another approach, Hsieh et al. successfully covalently conjugated PSs (Ir complexes) to alkyl dithiol molecules which bind to CdSe/ZnS.⁸ These complexes were tailored to have little spectral overlap to minimize FRET, and they could be employed for both imaging and therapy. Unfortunately, they were soluble only in methanol and thus could not be used in biological applications. To overcome these issues of water solubility, Shi et al. utilized charge interactions to assemble QD–photosensitizer nanocomposite materials using positively charged water-soluble CdTe QDs and negatively charged PSs.⁹ Applications for these

conjugates may be limited because of the inherent cytotoxicity of core-only Cd-based nanoparticles and the potential instability of charge-assembled complexes in the cellular environment.^{10,11}

Previously, it was shown that ZnS shells greatly reduce toxic effects of cadmium-based QDs in live cells and provide high quantum yield and photostability for long-term imaging.¹² Pinaud et al. used phytochelatin-related peptides to overcoat CdSe/ZnS, resulting in QDs with excellent colloidal and photophysical properties.¹³ Furthermore, this strategy gave the opportunity to covalently conjugate molecules of interest to peptides. Clear potential advantages of QD–PSs over PSs alone

(10) Derfus, A. M.; Chan, W. C. W.; Bhatia, S. N. *Nano Lett.* **2004**, *4*, 11.

(11) Tsay, J. M.; Michalet, X. *Chem. Biol.* **2005**, *12*, 1159.

(12) Kirchner, C.; Liedl, T.; Kudera, S.; Pellegrino, T.; Munoz, Javier, A.; Gaub, H. E.; Stolzle, S.; Fertig, N.; Parak, W. J. *Nano Lett.* **2005**, *5*, 331.

(13) Pinaud, F.; King, D.; Moore, H.-P.; Weiss, S. J. *Am. Chem. Soc.* **2004**, *126*, 6115.

(8) Hsieh, J. M.; Ho, M. L.; Wu, P. W.; Chou, P. T.; Tsaih, T. T.; Chi, Y. *Chem. Commun.* **2006**, 615.

(9) Shi, L. X.; Hernandez, B.; Selke, M. *J. Am. Chem. Soc.* **2006**, *128*, 6278.

include the larger absorption coefficients of QDs (together with the ability to efficiently transfer energy with PSs), the ability to target molecules of interest, imaging capabilities, and a large variety of schemes available to bioconjugate QDs. Here we show that peptide-coated QDs (pcQDs) can form extremely stable conjugates with PSs, which may be used as multifunctional probes for live cell targeting, imaging, and photodynamic therapy.

2. Materials and Methods

2.1. Chemicals. Rose bengal was purchased from VWR. *N*-Hydroxy succinimide (NHS), 1-ethyl-3-(3-dimethylaminopropyl)carbodiimide (EDC), 6-bromohexanoic acid, dimethylsulfoxide (DMSO), pyridine, cadmium oxide (CdO), dimethyl cadmium, diethyl zinc, trioctylphosphine oxide (TOPO), tributylphosphine (TBP), selenium powder, and deuterium dioxide D₂O were purchased from Aldrich. Chlorin e6 monoethylene diamine monoamide was purchased from Frontier Scientific (Logan, Utah). Peptides were purchased from Synpep.

2.2. Quantum Dot Synthesis. Green-emitting (538 nm) and red-emitting (620 nm) CdSe/CdS/ZnS QDs were synthesized using methods similar to those previously described.¹⁴ Both QD samples have quantum yields (QYs) > 20% in toluene and in water (coated with peptides without PSs).

2.3. Photosensitizer Conjugation to QDs. Rose bengal (RB) linked to an NHS ester was synthesized as described in a previous protocol.¹⁵ Conjugation of RB–NHS ester to QDs was achieved by first covalently coupling rose bengal to peptides, and then coating QDs with the modified peptides. Typically 0.5 mg of rose bengal ester was incubated with 1 mg of lysine-terminated peptides (K-G-S-E-S-G-G-S-E-S-G-Cha-C-C-Cha-C-C-Cha-C-C-Cha-C-C-Cha-Cmd) in 50 μ L of DMSO for 1 h. This solution was then co-incubated with peptides of other functionalities (PEG, biotin, lysine-terminated peptides, etc.)⁴ for a total of 4 mg of peptides. CdSe/CdS/ZnS QDs of emissions at either 538 nm or 620 nm (QY > 20%) were precipitated and redispersed in 450 μ L of pyridine. TMAOH (13 μ L) was added to the QD solutions to trigger the deprotonation of sulfhydryl groups and binding of peptides to the QD surfaces. QD–photosensitizer conjugates were run through a NAP 5 or NAP 10 column (Amersham Biosciences) and then dialyzed in PBS buffer at pH 7.4.

Chlorin e6 monoethylene diamine monoamide was successfully conjugated to QDs using similar methods. Decanedioic acid disuccinimidyl ester was synthesized to act as a homobifunctional linker with NHS ester on both ends by a minor modification of the known method.¹⁶ A 10-fold excess of these molecules was incubated with lysine-terminated peptides (Synpep) in 50 μ L of DMSO for 1 h to form peptide–NHS ester conjugates while avoiding cross-linking of lysine peptides. Amine-terminated chlorin e6 (Frontier Scientific) in molar excess twice that of NHS groups in solution was then incubated with this solution for 1 h to form peptide–chlorin e6 conjugates. The binding of these peptides to QDs was done according to what was described above. Alternatively, cysteine-terminated QDs (peptide sequence: C-G-S-E-S-G-G-S-E-S-G-Cha-C-C-Cha-C-C-Cha-C-C-Cha-Cmd) were incubated with SMCC (a heterobifunctional linker with a maleimide group and NHS ester) and the amine-functionalized chlorin e6. Although stable covalent conjugation occurred with this method, the reaction was detrimental to the photophysics of both the QD and the photosensitizer.

The number of PSs conjugated to QDs was controlled by changing the stoichiometry of photosensitizer-conjugated peptides to peptides of other functionalities before binding them to QDs. This enabled us

to control the stoichiometry in the range of 1–30 PSs per QD. More PSs could be bound to the larger QDs because of their larger surface area. All samples were stored in the dark at 4 °C after the completion of the reactions and purification procedures.

2.4. UV/Vis Absorption and Photoluminescence Detection. The photoluminescence emissions of the QD–photosensitizer conjugates were detected using a fluorimeter (photon technologies international) equipped with a Hamamatsu R928 photomultiplier tube (PMT) and excited with a 75-W Xe lamp. UV/vis absorption spectroscopy was performed using a Perkin-Elmer Lambda 25 UV/vis spectrometer.

Details of QD:PS ratio calculations are provided in the Supporting Information.

2.5. Fluorescence Lifetime Measurements. Lifetime measurements were conducted using a home-built confocal microscope with a 100 \times objective (Zeiss 100 \times Apochromat, NA 1.4). Samples were excited by a picosecond-pulsed 467-nm laser (LDH-P-C-470, PicoQuant GmbH, Berlin), synchronized to a 5 MHz source from the laser driver (PDL-800B, PicoQuant GmbH, Berlin), detected with single-photon avalanche detectors (SPCM-AQR-14, Perkin-Elmer), and timed using a TCSPC board (SPC-630, Becker and Hickl GmbH). Band-pass filters were used for detection (green with 520DF40 and red with 580AF60, Omega Optical). Lifetime decay curves were fit to a sum of three exponents as previously demonstrated by Dahan et al.¹⁷ Only a tri-exponential function yielded acceptable fits to our fluorescence lifetime decay curves.

2.6. Singlet Oxygen Measurements. **2.6.1. Chemical Detection.** QD–photosensitizer conjugates were run with D₂O through a Nap 5 column and then a G25 spin column to purify from excess peptides and PSs. These solutions were then incubated with anthracene dipropionic acid (APA) which is used for chemical detection of singlet oxygen.¹⁸ As singlet oxygen is generated, APA converts to its endoperoxide form, which in turn leads to its photodestruction (photobleaching). Bleaching was monitored by measuring the reduction in absorption (at the APA absorption peak, 400 nm). The reduction in absorption was monitored as function of time after irradiating samples with different wavelengths using a Xe lamp equipped with a monochromator.

2.6.2. Spectroscopic Detection. Quantum yields of singlet oxygen generated from purified QD–photosensitizer conjugates dispersed in D₂O were achieved with a Nd:YAG laser at an excitation wavelength of either 355 nm or 532 nm (New Wave Research Mini-Laser II). Singlet oxygen luminescence decay signals were recorded on a 500-MHz oscilloscope (LeCroy 9350 CM) and fitted to a first-order exponential function on Origin 6.0. The generated singlet oxygen was plotted as a function of optical density of QD–PSs. This plot was fit and compared to a plot of methylene blue as a standard to measure singlet oxygen quantum yields. The optical densities of the solutions were recorded on a Vary 300 Bio spectrometer.

2.7. Calculations for FRET efficiency. In the Förster formalism, E , the FRET efficiency between a single donor–acceptor (D–A) pair, is given by:

$$E = \frac{k_{\text{FRET}}}{k_{\text{FRET}} + \tau_{\text{D}}} = \frac{R_0^6}{R_0^6 + r^6} \quad (1)$$

where k_{FRET} is rate of FRET, τ_{D} is the intrinsic donor lifetime (in the absence of acceptor), R_0 (Förster radius) is D–A distance at which the transfer efficiency is 50%, and r is the D–A distance. The FRET efficiency increases when the number of acceptors (n) per QD increases as previously described in Clapp et al.¹⁹

(14) Tsay, J. M.; Doose, S.; Pinaud, F.; Weiss, S. *J Phys. Chem. B* **2005**, *109*, 1669.

(15) Conlon, K. A.; Berrios, M. J. *Photochem. Photobiol.*, **2001**, *65*, 22.

(16) Hill, M.; Bechet, J.; d'Albis, A. *FEBS Lett.* **1979**, *102*, 282.

(17) Dahan, M.; Laurence, T.; Pinaud, F.; Chemla, D. S.; Alivisatos, A. P.; Sauer, M.; Weiss, S. *Opt. Lett.* **2001**, *26*, 825.

(18) Lindig, B. A.; Rodgers, M. A. J.; Schaap, A. P. *J. Am. Chem. Soc.* **1980**, *102*, 5590.

(19) Clapp, A. R.; Medintz, I. L.; Mauro, J. M.; Fisher, B. R.; Bawendi, M. G.; Mattoussi, H. *J. Am. Chem. Soc.* **2004**, *126*, 301.

$$E = \frac{nR_0^6}{nR_0^6 + r^6} \quad (2)$$

R_0 can be calculated using the following equation:

$$R_0 = \left(\left(\frac{9000(\ln 10)\kappa_p^2 Q_D}{N_A 128\pi^5 n_D^4} \right) I \right)^{1/6} \quad (3)$$

where:

$$I = \int_0^\infty PL_{D-\text{con}}(\lambda)\lambda^4 d\lambda \quad (4)$$

and:

$$\kappa_p^2 = 2/3 \quad (5)$$

In these equations, I is the overlap integral which measures the amount of spectral overlap between the donor emission and the acceptor absorbance, κ_p^2 is the orientation factor, and n_D is the refractive index of the solvent. In the work of Clapp et al., $\kappa_p^2 = 2/3$, a value for randomly oriented dipoles, was assumed for FRET in quantum dot–dye conjugates. This was justified from the assumption that quantum dots have symmetric excitonic wavefunctions around their centers.¹⁹ We use the same assumptions in this work, as it is the best available treatment for our system. It is also assumed that the dipoles of the photosensitizers are completely random around the quantum dot because they should be free to rotate on a flexible peptide.

3. Results and Discussion

3.1. Nonspecific Attachment of PSs to QDs. In a first approach to create QD–photosensitizer conjugates, nonspecific adsorption of photosensitizer molecules to pcQD surfaces was attempted by incubating positively charged rose bengal with QDs in various concentrations. The rationale behind this approach was that positively charged PSs should form complexes with negatively charged QDs through electrostatic interactions. Although quenching of the fluorescence of QDs was observed with increasing rose bengal concentrations, the rose bengal fluorescence did not increase, showing that FRET did not occur. Furthermore, after purification using a size exclusion column (G 25 beads), unmodified pcQDs were isolated with no trace of rose bengal, proving that this was not a stable conjugate.

Binding of PSs through ligand interactions with the QD surfaces was also attempted. Chlorin e6, a well-studied photosensitizer absorbing in the far-red region (654 nm), was modified by an alkylamine linker (Frontier Scientific) and incubated with pcQDs for an hour. We expected that if cysteines on the peptides did not completely coordinate all atoms on the surface it would be possible for alkyl amine groups to also bind to the QD surfaces. However, as was the case for RB–QD samples, chlorin e6–QD samples did not form stable conjugates, and with purification through a size exclusion column, the PSs were released from the QD surface. The instability of these noncovalent conjugation strategies necessitated a more robust way of binding PSs to QDs.

3.2. Covalent Attachment of PSs to QDs. Conjugation of PSs, such as rose bengal and far-red-absorbing chlorin e6, to QDs was accomplished by covalently bonding PSs to phytochelatin-related peptides before their exchange with surfactants. In the case of rose bengal, the NHS ester group was added to the molecules by reacting with 6-bromohexanoic acid, *N*-

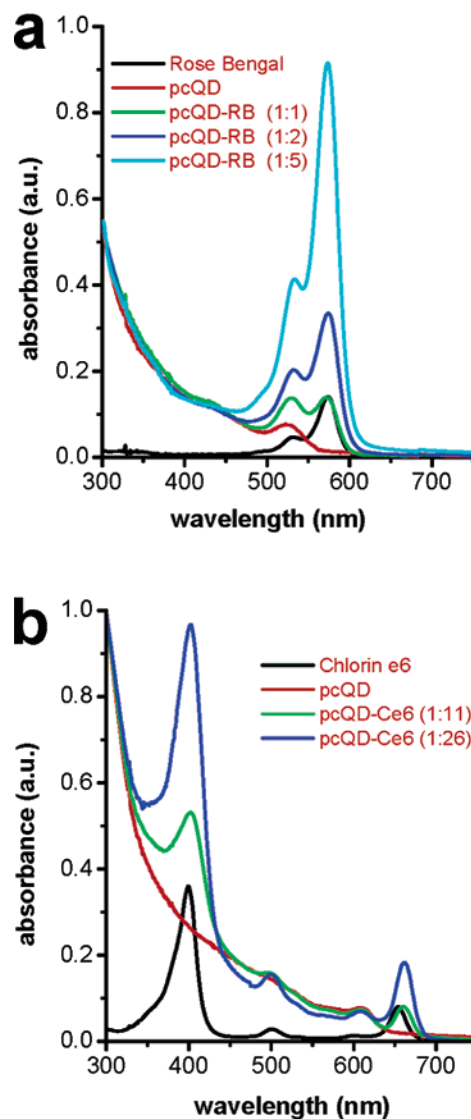


Figure 3. UV/vis absorption spectra of (a) 545-nm emitting pcQDs conjugated to rose bengal at ratios of ~1:1, 1:2, and 1:5 and (b) 628-nm emitting pcQDs conjugated to chlorin e6 at ratios 1:11 and 1:26

hydroxy succinimide (NHS), and 1-ethyl-3-(3-dimethylamino-propyl)carbodiimide (EDC). Subsequently, these molecules were attached to lysine-terminated peptides by incubating them in DMSO (Figure 1). In the case of chlorin e6 attachment to QDs, a molecule with NHS esters at two ends of an alkyl chain was synthesized. This molecule was reacted first with the lysine peptides and then with amine-modified chlorin e6 (Figure 2). The peptide exchange on QDs with modified peptides was then accomplished using a similar scheme developed by Pinaud et al.¹³ Both these strategies resulted in very robust and stable covalent conjugation which did not affect the photophysical properties of the PSs and QDs. After various purification procedures including size exclusion column filtration and dialysis, conjugates were colloidal and photophysically stable for months in water, D₂O, and aqueous buffer when stored in the dark at 4 °C. Figure 3 shows absorption spectra of QDs attached to PSs rose bengal (a) and chlorin e6 (b) after purification. Important to note is the ability to control the stoichiometry of PSs on QDs (in the range of 1–30 PS per QD). This was achieved by mixing different amounts of peptides with different functionalities in the same peptide-coating reac-

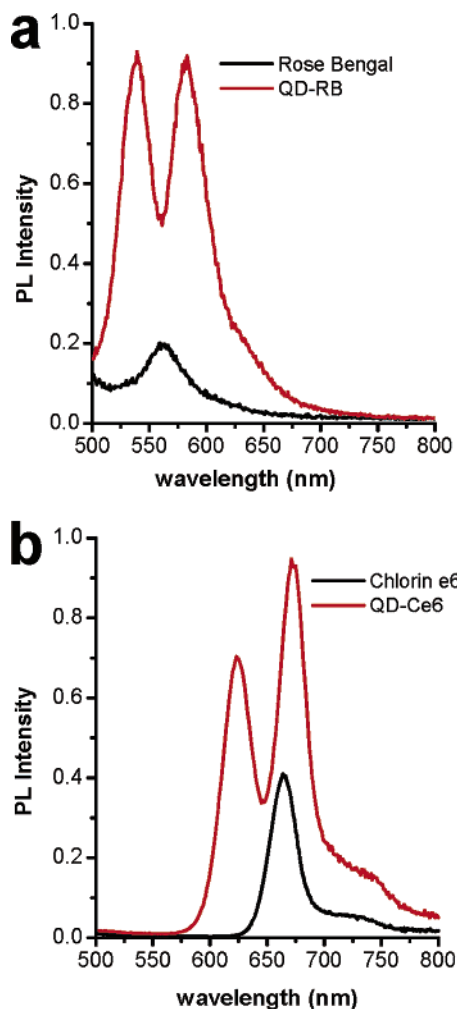


Figure 4. Photoluminescence spectra of (a) rose bengal conjugated QDs (red) and rose bengal alone (black) excited at 450 nm with equal concentrations of rose bengal. (b) Chlorin e6-conjugated QDs (red) and chlorin e6 alone (black) excited at 450 nm with equal concentrations of chlorin e6

tion.^{4,13} Using QDs of different sizes/surface areas also controlled the number of PSs bound to each QD. Through this method, we were able to bind peptides with PSs, biotin, and PEG all on the same QDs. Fluorescence correlation spectroscopy results showed a difference of $\sim 4\text{--}5$ nm in the hydrodynamic diameters between lysine-terminated, peptide-coated QDs and chlorin e6 peptide-coated CdSe/CdS/ZnS QDs, as expected from the length of the alkyl linkers and the size of the photosensitizer (data not shown). They also showed only minimal aggregation, demonstrating that conjugation did not adversely affect the colloidal properties of pcQDs.

3.3. Fluorescence Resonance Energy Transfer between QDs and PSs. It was previously reported that FRET can be an efficient process between QDs and dyes, including PSs.^{7,20} In this section, we also show evidence for FRET between QDs (acting as donors) and PSs (acting as acceptors). With the covalent conjugation schemes described above, rose bengal and chlorin e6 were stably attached to QDs. Figure 4 shows the dramatic increase of fluorescence of both rose bengal (attached to green QDs) and chlorin e6 (attached to red QDs) as a result

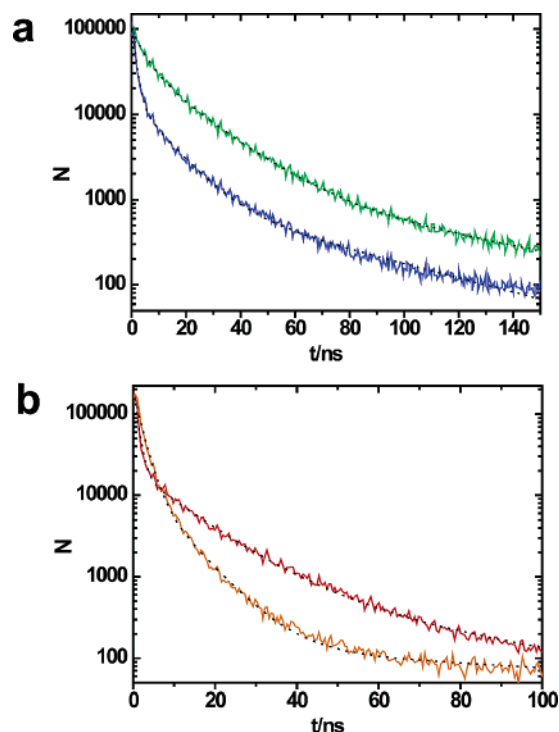


Figure 5. Fluorescence lifetime decay curves of (a) green-emitting pcQDs alone (green) and conjugated to rose bengal (blue), and (b) red-emitting pcQDs alone (red) and conjugated to chlorin e6 (orange). Dashed lines correspond to fits to an exponential function with three components.

of FRET (red curves) in comparison with fluorescence of PSs alone at the same concentration (black curves). This observation was accompanied by a decrease in photoluminescence intensity of the QDs ($>90\%$ loss compared with that of green-emitting pcQDs with no PSs). The QD–photosensitizer conjugates were excited at 450 nm, a wavelength at which both rose bengal and chlorin e6 have very little absorption and both red and green QDs have a substantial amount of absorption (see Figure 3).

Fluorescence lifetime measurements confirmed that both QD–RB and QD–chlorin e6 conjugates undergo FRET. Fluorescence lifetime decay curves of green-emitting QDs with and without the conjugation to rose bengal show the drastic shortening of the fluorescence lifetimes of pcQDs upon conjugation to photosensitizer acceptors as expected from the FRET process (Figure 5a). Likewise, the fluorescence lifetime of red-emitting QDs upon covalent conjugation to chlorin e6 is shortened (Figure 5b). Table 1 lists the time constants extracted from fitting the fluorescence lifetime decay curves on QDs and QD–photosensitizer conjugates to a triple exponential function. The shortest lifetime component of green QDs decreases from 4 to 1 ns and increases in contribution from 58% to 89%. It can also be clearly seen that the second lifetime components for both green- and red-emitting QDs shorten upon respective conjugation to rose bengal and chlorin e6.

In the case of green-emitting QDs conjugated to rose bengal, it was calculated that the R_0 value (50% FRET efficiency) was ~ 45 Å.²¹ This distance was approximately the same as the distance between QD (donor) and rose bengal (acceptor), taking into account the size of the QD (5 nm), the peptides, and the rose bengal linker, making the FRET process efficient. To

(20) Medintz, I. L.; Clapp, A. R.; Mattoussi, H.; Goldman, E. R.; Fischer, B.; Mauro, J. M. *Nat. Mater.* **2003**, *2*, 630.

(21) Lakowicz, J. R. *Principles of Fluorescence Spectroscopy*, 2nd ed.; Plenum Press: New York, 1999.

Table 1. Time Constants and Their Contributions Extracted from Fitting Fluorescence Lifetime Decay Measurements Performed on Green QDs, Green QD–Rose Bengal (RB) Conjugates (1:5), Red QDs, and Red QD–Chlorin e6 Conjugates (1:26)

	green QD	green QD+RB	red QD	red QD+Chl e6
donor lifetime 1 (ns)	73.4	52.4	49.3	145
lifetime	0.016	0.008	0.004	0.005
1 amp fraction				
donor lifetime 2 (ns)	16.6	10.6	11.8	7.70
lifetime	0.403	0.096	0.074	0.076
2 amp fraction				
donor lifetime 3 (ns)	4.31	1.30	1.05	1.93
lifetime	0.580	0.893	0.922	0.923
3 amp fraction				

decrease optimal spectral matching for FRET, red-emitting QDs were conjugated to rose bengal, and with excitation of the QDs at 450 nm, the PL of QDs remained intact, while rose bengal did not show any fluorescence enhancement (data not shown).

In contrast to the green QD–RB conjugates, the red QD–chlorin e6 conjugates were characterized by a relatively inefficient FRET process but retained the photoluminescence of the QD. The red QD–chlorin e6 conjugates had a calculated R_0 value of ~ 44 Å, but the average distance between the center of the QD and the chlorin e6 was expected to be ~ 75 Å (due to the increased size of the QD and linker molecule) giving only $\sim 10\%$ FRET efficiency.²¹ Although this FRET efficiency was low, the exciton absorption peak of 610 nm of red-emitting QDs is approximately $10\times$ greater than the absorption peak of conjugated chlorin e6 at 654 nm, meaning that there is a possibility that large amounts of singlet oxygen may still be generated while retaining sizable unquenched QDs emission (that could be used for imaging). Furthermore, by adding up to 26 chlorin e6 molecules to each red-emitting QD, the calculated FRET efficiency using eq 2 was increased to 50%. Experimentally, it was determined that, as expected, a large amount of quenching occurred to the QD fluorescence of red QDs with the addition of more PSs. This fluorescence was recovered after the PSs were photobleached, and subsequently, the QDs remained photostable under UV irradiation.

These results suggest that the amount of FRET between QDs and PSs may possibly be tailored for different applications. For instance, by limiting FRET, QDs may be used for both imaging and PDT at the same time by exciting at either one wavelength (using FRET) or two different wavelengths (no FRET). By utilizing a highly efficient FRET process, the QDs would only be weakly fluorescent (because of energy transfer), but the PDT efficacy may increase significantly because of the larger absorption cross section of the QD. Alternatively, QD–photosensitizer conjugates with relatively inefficient FRET processes could still deliver PDT effectively because of the high absorption cross sections of QDs, and the QD would have minimal loss of fluorescence. Finally, by exciting at two different wavelengths altogether with spectrally unmatched QDs and PSs, the QD–photosensitizer conjugates could be used to image and deliver PDT, but would not take advantage of the higher absorption cross sections of QDs. The FRET efficiency between QD and photosensitizer may be tuned by choosing QD donors and PS acceptors with the appropriate amount of spectral overlap and by changing the distance between the donor (QD)

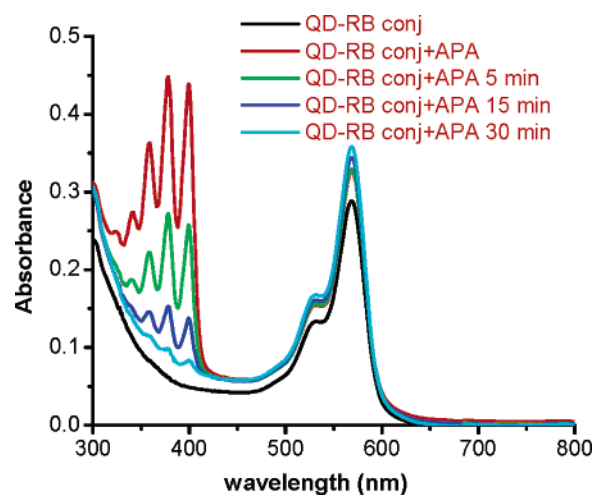


Figure 6. UV/vis absorption spectra of rose bengal conjugated QDs incubated with anthracene dipropionic acid, irradiated at 570 nm for various time intervals

and acceptor (photosensitizer). This can be done by varying the sizes of the QDs, by varying the size of linkers between QDs and PSs, and finally by altering the amount of PSs bound to the QD surface.

3.4. Detection of Singlet Oxygen from QD–Photosensitizer Conjugates. According to Samia et al. a small amount of singlet oxygen was generated by CdSe QDs dispersed in toluene.⁷ While it might be possible to improve singlet oxygen yield by engineering the photophysical properties of QDs, currently this yield is not high enough for effective PDT. We determined that there was no detectable amount of singlet oxygen generated from our peptide-coated QDs alone using the anthracene dipropionic acid (APA) assay. This assay was done on various structures of QDs including type I CdSe, CdSe/CdS/ZnS,¹⁴ and type II, CdTe/CdSe QDs.²² We instead chose to develop QDs as PS carriers with the potential for improved singlet oxygen yield, improved PDT efficacy (through FRET), and the potential to simultaneously act as imaging and therapeutic agents.

In contrast to these findings, our QD–photosensitizer conjugates were found to produce singlet oxygen both by exciting the conjugates at the PS excitation and through the FRET mechanism. For example, the APA assay was employed for green QD–RB conjugates with excitation at rose bengal's absorption peak (565 nm). Figure 6 shows the extensive bleaching of APA as function of time (amplitude reduction of spectral features around 350–400 nm) when incubated with QD–RB conjugates (QD:RB = 1:5) in D₂O and irradiated with 570-nm light. Control experiments with only APA and using the same excitation showed no bleaching. Similar results of singlet oxygen detection using this assay were found for QD–chlorin e6 conjugates with excitation near their absorption peak.

A more direct way for quantifying singlet oxygen generation from PSs is the spectroscopic detection of singlet oxygen's phosphorescence. Detection of singlet oxygen generated from QD–photosensitizer conjugates was accomplished by excitation with a Nd:YAG laser at 532 and 355 nm, and phosphorescence was detected at 1270 nm with a liquid nitrogen-cooled Germanium photodiode detector. Singlet oxygen quantum yields were measured as high as 0.17 for QD–RB conjugates and as high

(22) Kim, S.; Fisher, B.; Eisler, H.-J.; Bawendi, M. *J. Am. Chem. Soc.* **2003**, *125*, 11466.

Table 2. Singlet Oxygen Quantum Yields of Various QD–Photosensitizer Samples Using Phosphorescence Detection of Singlet Oxygen at 1270 nm

QD–PS conjugate	singlet oxygen QY 355 nm	singlet oxygen QY 532 nm
green QD–RB (1:1)	0.17	0.09
green QD–RB (1:5)	0.14	0.05
red QD–chlorin e6 (1:26)	0.10	0.31

as 0.31 for QD–chlorin e6 conjugates (see Table 2). These yields are reduced compared to the yields of unconjugated PSs. This reduction could be due to several factors including the direct excitation of the photosensitizer, inefficiency of the FRET mechanism, and quenching or loss of intersystem crossing in PSs due to the conjugation reactions between QD and PS. Since most of the absorption at 355 nm is due to the QD (as opposed to the photosensitizer), we suggest that the main limiting factor for singlet oxygen quantum yields is an inefficient FRET mechanism, i.e., the amount of spectral overlap of the donor emission to the acceptor absorption, and the donor–acceptor distance. Conversely, there should be a significant amount of direct excitation of the sensitizer at 532 nm. For the RB–QDs, quantum yields at this wavelength appear to be slightly lower compared to those at excitation at 355 nm. This suggests that the main pathway of singlet oxygen production is via a FRET mechanism. The quantum yield of singlet oxygen via direct excitation of a photosensitizer is the product of the triplet quantum yield, the fraction of triplet excited sensitizer quenched by dioxygen, and the fraction of triplet oxygen involved in the quenching process that is excited to the singlet state.^{23,24} Since the quantum yields at 532 nm are much lower than those of the free sensitizer, the attachment of the photosensitizer to the QD inhibits intersystem crossing to the sensitizer or the triplet excited sensitizer is efficiently quenched by the ground-state QD or excitation of the triplet oxygen involved in the quenching process is prevented by the QD. If there were an efficient quenching process of the triplet excited sensitizer in competition with quenching of the sensitizer by triplet oxygen, increasing the oxygen concentration in solution could possibly increase the singlet oxygen quantum yield. The exact reasons why the

(23) Wang, S. Z.; Gao, R. M.; Zhou, F. M.; Selke, M. *J. Mater. Chem.* **2004**, *14*, 487.

(24) Schweitzer, C.; Schmidt, R. *Chem. Rev.* **2003**, *103*, 1685.

directly excited sensitizer attached to the QD produces singlet oxygen less efficiently than the free sensitizer is unclear at the moment.

The behavior of the QD–chlorin e6 complex is clearly different. The quantum yield from indirect excitation (355 nm) is lower than that for the RB–QD species, consistent with the diminished FRET of this species. On the other hand, the quantum yield from direct excitation at 532 nm is much higher (0.31). It appears that the diminished photophysical interactions between the QD and sensitizer of this species lead to a much greater quantum yield by direct excitation of the sensitizer. If this trend were general, it might be advantageous to use QDs for imaging and the sensitizer for direct excitation, and attach sensitizers such that photophysical interactions between the two are limited. More quantum dot–sensitizer hybrids need to be studied in detail to determine if this is a general trend. Experiments in this direction are in progress.

Conclusions

We have shown that water-stable, peptide-coated QD–photosensitizer conjugates can be synthesized without deteriorating the photophysical properties of both the QDs and photosensitizers. Furthermore, the conjugates could efficiently generate singlet oxygen for PDT either through direct excitation of PSs or through the FRET mechanism. Future work will focus on covalently coupling QD–photosensitizer conjugates with targeting biomolecules and demonstrating targeting, imaging, and photodynamic therapy in live animals.

Acknowledgment. We thank Fabien Pinaud, Erol Basic, and Laurent Bentolila for their helpful suggestions. This work was supported by NIH Grant 5-R01-EB000312, the Jonsson Comprehensive Cancer Center multidisciplinary grant and the NSF, The Center for Biophotonics, an NSF Science and Technology Center managed by the University of California, Davis, under Cooperative Agreement PHY0120999. M.S. and L.S. gratefully acknowledge support from the NSF-PREM Program (Award No. 0351848).

Supporting Information Available: Singlet oxygen phosphorescence decay curves of QD–RB conjugates. This material is available free of charge via the Internet at <http://pubs.acs.org>.

JA070713I